

## Identification and Robust $H_\infty$ Control of the Rotational/Translational Actuator System

Mahdi Tavakoli, Hamid D. Taghirad, and Mehdi Abrishamchian

**Abstract:** The Rotational/Translational Actuator (RTAC) benchmark problem considers a fourth-order dynamical system involving the nonlinear interaction of a translational oscillator and an eccentric rotational proof mass. This problem has been posed to investigate the utility of a rotational actuator for stabilizing translational motion. In order to experimentally implement any of the model-based controllers proposed in the literature, the values of model parameters are required which are generally difficult to determine rigorously. In this paper, an approach to the least-squares estimation of the parameters of a system is formulated and practically applied to the RTAC system. On the other hand, this paper shows how to model a nonlinear system as a linear uncertain system via nonparametric system identification, in order to provide the information required for linear robust  $H_\infty$  control design. This method is also applied to the RTAC system, which demonstrates severe nonlinearities due to the coupling from the rotational motion to the translational motion. Experimental results confirm that this approach can effectively condense the whole nonlinearities, uncertainties, and disturbances within the system into a favorable perturbation block.

**Keywords:** Rotational/translational actuator, nonlinear system identification, system parametric identification, least squares estimation, nonparametric identification, prediction error method, unmodelled dynamics, model uncertainty, linear uncertain system, robust  $H_\infty$  control.

### NOMENCLATURE

Air viscous coefficient  $c$

Arm angular position  $\theta$

Arm angular velocity  $\dot{\theta}$

Arm eccentricity  $e$

Arm inertia  $I$

Arm mass  $m$

Arm rotation viscous coefficients  $K_{v1}, K_{v2}$

Backward shift operator  $q^{-1}$

Cart mass  $M$

Cart translation Coulomb coefficient  $d$

Cart translational position  $q$

Cart translational velocity  $\dot{q}$

Complementary sensitivity transfer function  $T(s)$

Controller transfer function  $C(s)$

Coupling parameter  $\varepsilon$

Current-to-torque gain  $K_m$

Disturbance force  $F$

Expectation operator  $E$

Kronecker delta  $\delta_{t,s}$

Model input  $u(t)$

Model output  $y(t)$

Model parameter vector  $\Theta$

Motor current  $i$

Motor torque  $N$

Noise covariance matrix  $\Lambda$

Nominal system transfer function  $P_0(s)$

Normalized cart position  $\xi$

Normalized cart velocity  $\dot{\xi}$

Normalized disturbance force  $w$

Normalized motor torque  $u$

Observation vector  $Q$

Perturbation  $\Delta$

Predicted output  $\hat{y}(t; \theta)$

Prediction error  $\eta(t, \theta)$

Manuscript received August 17, 2004; revised March 15, 2005; accepted June 29, 2005. Recommended by Editorial Board member Seung-Hi Lee under the direction of Editor-in-Chief Myung Jin Chung.

Mahdi Tavakoli is with the Department of Electrical and Computer Engineering, University of Western Ontario, London, Ontario N6A 5B9, Canada (e-mail: tavakoli@uwo.ca).

Hamid D. Taghirad is with the Department of Electrical Engineering, K. N. Toosi University of Technology, P.O.Box 16315-1355, Tehran, Iran (e-mail: taghirad@kntu.ac.ir).

Mehdi Abrishamchian is with Maxtor Corporation, Shrewsbury, MA, USA (e-mail: mehdi\_abrishamchian@maxtor.com).

Regressed variables vector  $\Theta$   
 Regressor matrix  $\Phi$   
 Sensitivity transfer function  $S(s)$   
 Spring stiffness  $k$   
 Spring viscous coefficient  $b$   
 System transfer function  $P(s)$   
 Uncertainty weighting transfer function  $W(s)$   
 White noise  $e(t)$

## 1. INTRODUCTION

The Rotational/Translational Actuator (RTAC) experiment has originally been studied as a simplified model of a dual-spin spacecraft. It has been shown that this system is mathematically and qualitatively equivalent to a dual-spin spacecraft, i.e., they have similar averaged equations and exhibit similar dynamic behaviors [1]. One important issue with regard to the control of dual-spin spacecrafts is the *resonance capture phenomenon*<sup>1</sup>. As a result of the similarities, spacecraft control strategies aimed at minimum-effort stabilization while avoiding resonance capture can first be tried on the RTAC system which possesses all essential characteristics of the spacecraft dynamic behavior [1].

Later, the RTAC system has been studied to investigate the usefulness of a rotational actuator for stabilizing translational motion [2]. In this nonlinear system, unlike a linear actuator, the actuator stroke limitations are implicitly involved in the system dynamics [3]. Consider the translational oscillator with an eccentric rotational proof mass shown in Fig. 1. The oscillator consists of a cart of mass  $M$  connected to a fixed wall by a linear spring of stiffness  $k$ . The motion is confined in one direction and is merely in the horizontal plane so that gravitational forces do not contribute. The proof mass attached to the cart has mass  $m$  and moment of inertia  $I$  about its center of mass, which is located at a distance  $e$  from the point about which the proof mass rotates.  $N$  denotes the control torque applied by the rotational actuator to the proof mass, and  $F$  is the disturbance force on the cart.

In this nonlinear benchmark problem, the control objective is the oscillator stabilization despite external disturbances via the control torque provided by the rotational actuator. More specifically, it is required to design a controller such that:

- The closed-loop system is stable.
- The closed-loop system exhibits good settling behavior for a class of initial conditions.
- The closed-loop system exhibits good disturbance rejection compared to the uncontrolled oscillator for

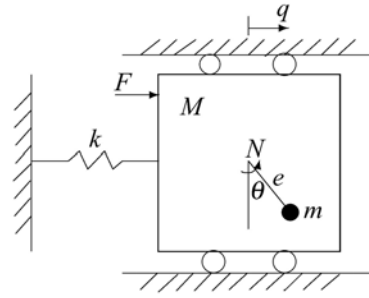


Fig. 1. Rotational actuator to control a translational oscillator.

- a class of disturbance signals.
- The control effort is feasible.

A number of research works are reported on this problem. For instance, Bupp, Bernstein and Coppola implement four nonlinear controllers on the RTAC, including an integrator back-stepping controller and three passivity-based controllers [4]. Also Jankovic, Fontaine and Kokotovic design and compare linear cascade controllers and passivity-based controllers for the system [5]. Kanellakopoulos and Zhao design a back-stepping controller for tracking [6], and Jiang and Kanellakopoulos design an output feedback controller through observer/controller back-stepping design [7]. Mracek and Cloutier use the state-dependent Riccati equation technique to produce a nonlinear controller for the benchmark problem [8]. Kolmanovsky and McClamroch propose a hybrid feedback control law expressed in terms of a continuous feedback part and a part including switched parameters [9]. Haddad and Chellaboina apply their method of designing nonlinear fixed-order dynamic passive controllers to the RTAC system [10]. Dussey and El-Ghaoui develop a measurement-scheduled output-feedback controller with an LMI approach for the system [11]. Tsiotras, Corless and Rotea use the theory of  $L_2$  disturbance attenuation to obtain solutions to the RTAC problem [12].

To implement any of the above-mentioned model-based controls in practice, it is necessary to have the values of the system parameters. While rigorous determination of the parameters of the actual system is quite difficult, this paper proposes a least-squares method for estimation of the parameters of this system and similar dynamical systems. On the other hand, the stated control objectives are very well suited for the linear robust control of the system. The second contribution of this paper is an identification-based method for representing the experimental RTAC system as a nominal linear system in addition to an uncertainty block, as required by the linear  $H_\infty$  control synthesis.

This paper is organized as follows. In Section 2, the nonlinear equations of motion and the system linearization around an equilibrium point are

<sup>1</sup>The attraction of a system into a state of sustained resonance.

discussed. Section 3 describes the experimental setup which realizes the equations of motion of the nonlinear system. Section 4 addresses the least-squares estimation of the system parameters aimed at model-based control. In Section 5, the time-domain nonparametric identification of the system suited for the  $H_\infty$  synthesis framework is discussed.

## 2. SYSTEM MODELLING

Let  $q$  and  $\dot{q}$  denote the translational position and velocity of the cart, and let  $\theta$  and  $\dot{\theta}$  denote the angular position and velocity of the rotational proof mass (Fig. 1). Assuming that the system shown in Fig. 1 operates in a horizontal plane, the equations of motion for the system are given as:

$$(M + m)\ddot{q} + kq = -me(\ddot{\theta} \cos \theta - \dot{\theta}^2 \sin \theta) + F, \quad (1)$$

$$(I + me^2)\ddot{\theta} = -me\ddot{q} \cos \theta + N. \quad (2)$$

With some transformations [2], the nondimensionalized state equations of the system are given by

$$\dot{\mathbf{x}} = \mathbf{f}(\mathbf{x}) + \mathbf{g}(\mathbf{x})u + \mathbf{d}(\mathbf{x})w, \quad (3)$$

where

$$\mathbf{f}(\mathbf{x}) = \begin{pmatrix} x_2 \\ x_2 \frac{-x_1 + \varepsilon x_4^2 \sin x_3}{1 - \varepsilon^2 \cos^2 x_3} \\ x_4 \frac{\varepsilon \cos x_3 (x_1 - \varepsilon x_4^2 \sin x_3)}{1 - \varepsilon^2 \cos^2 x_3} \end{pmatrix}^T,$$

$$\mathbf{g}(\mathbf{x}) = (0 \quad -\varepsilon \cos x_3 \quad 0 \quad 1)^T / (1 - \varepsilon^2 \cos^2 x_3),$$

$$\mathbf{d}(\mathbf{x}) = (0 \quad 1 \quad 0 \quad -\varepsilon \cos x_3)^T / (1 - \varepsilon^2 \cos^2 x_3).$$

Here,  $\mathbf{x} = (x_1 \quad x_2 \quad x_3 \quad x_4)^T = (\xi \quad \dot{\xi} \quad \theta \quad \dot{\theta})^T$ , where  $\xi$  is the normalized cart position, and  $u$  and  $w$  represent the normalized control torque and disturbance, respectively. In (3), the differentiation is performed with respect to the normalized time  $\tau$ . The parameter  $\varepsilon = me/\sqrt{(I + me^2)(M + m)}$  represents the coupling between the translational and rotational motions.

The above formulation of the RTAC experiment does not account for the effects of friction and spring damping which do exist in practice. The air friction and spring damping can be considered as disturbances on the cart, and may be modelled as viscous frictions with coefficients  $b$  and  $c$ , respectively. Therefore, (1) becomes

$$(M + m)\ddot{q} + kq + b\dot{q} = -me(\ddot{\theta} \cos \theta - \dot{\theta}^2 \sin \theta) - c\dot{q}.$$

The equilibrium point is  $\mathbf{x}_e = (0 \quad 0 \quad \theta_0 \quad 0)^T$  and  $u_e = 0$ , where  $\theta_0$  is any arbitrary value, provided the disturbance  $w$  is zero. Using Jacobians for this equilibrium point, the transfer function from the normalized torque  $u$  to the normalized cart position  $\xi$  is found to be

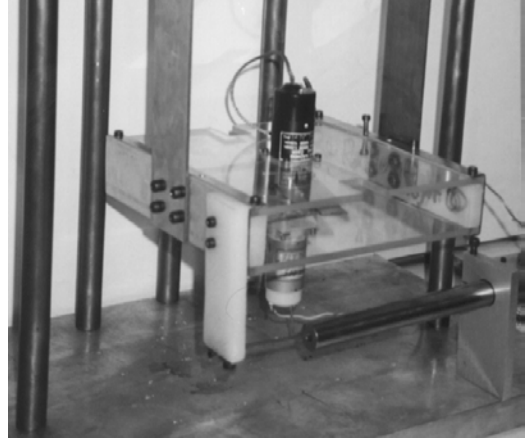


Fig. 2. The RTAC setup.

$$\frac{\Xi(s)}{U(s)} = \frac{\varepsilon \cos \theta_0}{(\varepsilon^2 \cos^2 \theta_0 - 1)s^2 - \frac{\nu}{\sqrt{k(M+m)}}s - 1}, \quad (4)$$

where  $\nu = b + c$ . This transfer function has a DC gain that varies with  $\theta_0$ , however, the poles are fairly insensitive to the variations of  $\theta_0$ . The term  $\cos \theta_0$  in the numerator implies that the pendulum vibrations about  $\theta = 0$  have the most influence on the cart displacement, while at  $\theta = 90^\circ$  they have the least effect.

## 3. EXPERIMENTAL TESTBED

The experimental testbed, aimed to realize the model depicted in Fig. 1, is constructed (Fig. 2). The basis for this setup, which is provided by an aluminum plate, is connected to a rigid ceiling by five perpendicularly mounted steel bars. The spring is realized by two beams fastened to the ceiling. These beams also serve to suspend the cart made of acrylic plates in the air, in order to reduce the friction as much as possible<sup>2</sup>. Due to the setup rigidity, the cart translation is merely confined to one direction, and roll, yaw and pitch rotations are suppressed as well. A DC motor and a tachometer are centered on the lower and upper plates of the cart, with their shafts secured together through a coupling to avoid eccentricity. The same coupling also serves to hold the eccentric arm and the proof mass.

The control torque is provided by the DC motor. A PWM current drive controls, through a PI feedback loop, the torque applied by the motor on the eccentric arm. The angular position of the arm is determined by integrating the angular velocity readings from the

<sup>2</sup>To reduce the friction, an air-cushion table solution was originally proposed by Bupp, Bernstein and Coppola [2]. To alleviate the mechanical complexities associated with the air table, we built the system with flexible beams used to implement both the spring and the suspension [13].

tachometer. In order to determine the cart translational position, a linear variable differential transformer (LVDT) is utilized. It consists of a body which is mounted on the basis, and a core which is attached to the cart and travels within the body. Therefore, the cart travels are translated to a proportional voltage at the output terminals of the LVDT which is logged by a PCL-818 data acquisition card from Advantech.

#### 4. PARAMETRIC IDENTIFICATION FOR MODEL-BASED CONTROL

To implement any of the model-based controls such as [1,2,4-12], it is necessary to have the values of system parameters. Since it is not always easy to rigorously determine the values of model parameters, a scheme for estimating these parameters using the least-squares method is formulated below.

##### 4.1. Method

The system equations of motion can be viewed as a set of equations in which the system parameters are *regressed variables* (unknowns) and certain functions of the measured variables serve as *regressors*. The first equation of motion of the RTAC system can be written as

$$\frac{M+m}{k}\ddot{q} + \frac{v}{k}\dot{q} + \frac{d}{k}\text{sgn}(\dot{q}) + \frac{me}{k}(\ddot{\theta}\cos\theta - \dot{\theta}^2\sin\theta) = -q,$$

where  $v$  is due to the air friction and spring damping, and  $d$  is the Coulomb friction coefficient. In a "free-oscillation experiment", in which the motor is idle and the cart is subject to free oscillations due to its initial position, the term  $\ddot{\theta}\cos\theta - \dot{\theta}^2\sin\theta$  will be negligible. Therefore, at the  $i$ -th sampling time during an identification experiment:

$$\begin{aligned}\Phi_i\Theta &= -q_i, \\ \Phi_i &= (\ddot{q}_i \quad \dot{q}_i \quad \text{sgn}(\dot{q}_i)), \\ \Theta &= \left( \frac{M+m}{k} \quad \frac{v}{k} \quad \frac{d}{k} \right)^T.\end{aligned}$$

Therefore, the vector of regressed variables  $\Theta$  can be estimated through the least-squares method if we have measurements leading to the values of the regressor matrix  $\Phi = (\Phi_1 \dots \Phi_n)^T$  and the observation vector  $Q = (-q_1 \dots -q_n)^T$ :

$$\Theta = (\Phi^T\Phi)^{-1}\Phi^TQ. \quad (5)$$

A similar scheme can be used to find the rest of system parameters through a set of "forced-oscillation experiments" in which inputs are provided to the motor. Incorporating the rotational viscous friction into the second equation of motion, (1)-(2) can be

rewritten as

$$\begin{aligned}me(\ddot{\theta}\cos\theta - \dot{\theta}^2\sin\theta) &= -kq - (M+m)\ddot{q} - v\dot{q} - d\text{sgn}(\dot{q}), \\ me\ddot{q}\cos\theta - K_m i + K_{v1}u_{\theta}\dot{\theta} + K_{v2}u_{-\theta}\dot{\theta} &= -(I + me^2)\ddot{\theta},\end{aligned} \quad (6)$$

where  $i$  is the motor current,  $K_m$  is the motor torque constant, and  $K_{v1}$  and  $K_{v2}$  represent the coefficients of asymmetric viscous friction in the arm rotational motion. As discussed in the next section, (6) can be solved simultaneously with respect to the unknown parameters  $me$ ,  $K_m$ ,  $K_{v1}$  and  $K_{v2}$  once the other parameters have been estimated through the free-oscillation experiments.

A consistency measure has been defined as the ratio of standard deviation of the parameter estimates to their mean value. Through a comprehensive set of simulations and experiments, it has been empirically shown that if this measure is less than 30% for all parameter estimates, then the model based on the mean values of parameter estimates is in good agreement with the actual system [14]. With two sets of data (the free- and forced-oscillation experiments) and a subset of the parameters estimated using each of these data sets, more consistent parameter estimates will be found compared to the case that all of the parameters were estimated at one attempt.

##### 4.2. Experimental results

Using ten free-oscillation experiments obtained for different cart initial positions, the least-squares estimates of  $\frac{M+m}{k}$ ,  $\frac{v}{k}$  and  $\frac{d}{k}$  can be found using (5). To find  $\Phi$  and  $Q$ , the cart position data are logged and then filtered by a 9<sup>th</sup>-order Chebychev filter implemented using a zero-phase-distortion routine (Matlab function *filtfilt* [15]) to remove the measurement noise. The filtered cart position data are then differentiated to find  $\dot{q}$  and  $\ddot{q}$ . Since the least-squares estimation is done offline, the filtered cart position data are differentiated using the two-point central difference formula which is a non-causal and more accurate method. The least-square estimations of  $\frac{M+m}{k}$ ,  $\frac{v}{k}$  and  $\frac{d}{k}$  from the free-oscillation experiments are listed in Table 1(a). Weighing the acrylic plates, motor, tachometer and arm results in  $M+m=1.230$  kg, and therefore  $k=132.6$  N/m,  $v=0.5543$  and  $d=24\times 10^{-3}$ .

Twenty forced-oscillation experiments with different cart initial positions and arm initial angles are performed while the input amplitudes are swept from 50% to 100% of their maximum value. For the setup built in the laboratory,  $I+me^2$  is mathematically determined to be  $9.5\times 10^{-5}$ . Having obtained the estimates of  $M+m$ ,  $k$ ,  $v$  and  $d$  from the free-

Table. 1. From top to bottom: Least square parameter estimates from (a) the free-oscillation experiments, and (b) the forced-oscillation experiments; (c) RTAC system parameter estimates.

	$\frac{M+m}{k}$	$\frac{v}{k}$	$\frac{d}{k}$
Mean	$9.27 \times 10^{-3}$	$4.18 \times 10^{-3}$	$1.81 \times 10^{-4}$
$\frac{\text{Std.dev.}}{\text{Mean}}$	0.64 %	9.68 %	14.74 %

	$me$	$K_m$	$K_{v1}$	$K_{v2}$
Mean	$1.06 \times 10^{-3}$	$8.04 \times 10^{-2}$	$1.39 \times 10^{-4}$	$1.49 \times 10^{-4}$
$\frac{\text{Std.dev.}}{\text{Mean}}$	15.5 %	6.2 %	34 %	33 %

Total mass	$M + m$	1.23 kg
Arm inertia moment	$I + me^2$	950 g.cm <sup>2</sup>
Spring stiffness	$k$	132.6 N/m
Coupling parameter	$\varepsilon$	0.1
Torque constant	$K_m$	0.08 N.m/A

oscillation experiments, (6) can simultaneously be solved with respect to the parameters  $me$ ,  $K_m$ ,  $K_{v1}$  and  $K_{v2}$ . The estimates are listed in Table 1(b).

Small consistency measures for the parameters estimated through free- and force-oscillation experiments ensure a good match between the estimated mathematical model and the actual system. Estimated values of important system parameters are summarized in Table 1(c).

## 5. NONPARAMETRIC IDENTIFICATION FOR ROBUST $H_\infty$ CONTROL

The RTAC problem was originally posed as a nonlinear benchmark problem and, as a result, the previous research has relied on an ideal, non-dissipative and fixed nonlinear model of the system given (1) and (2). Such an approach, however, does not consider the unmodelled dynamics, parametric uncertainties, disturbances or other deviations from the nonlinear model which do exist in practice. Therefore, it is important to look for more realistic control strategies, such as robust control, that can effectively take into account the deviations of a system from the theoretical model. Interestingly, the stated control objectives for the RTAC problem, namely the internal stability, fast settling, and good disturbance rejection in spite of limited control effort, are well suited for the robust control framework.

### 5.1. Method

We propose to estimate a nonlinear system as a nominal linear system in addition to uncertainty, in

order to provide the information required for the linear  $H_\infty$  control synthesis. While the determination of the weighting functions representing the uncertainty level of a system is a problem with the robust control, we will use system identification to find out the nominal model in addition to the corresponding uncertainty level. This scheme for representing nonlinear systems has successfully been applied to the control of harmonic drives by one of the authors [16]. It is interesting to observe the capability of a similar approach in capturing the dynamics of the RTAC system, which has severe nonlinearities due to the coupling from the rotational motion to the translational motion through a sinusoidal term. The next subsections explain how system identification can be used to model a nonlinear system in the format required by the linear robust  $H_\infty$  control. For a unified system identification/robust control design, see [17,18] and the references therein.

### Prediction-error identification

To produce a linear frequency response estimate of a nonlinear system, prediction-error system identification can be performed. In the prediction-error method [19], a general model structure  $\mathcal{M}(\Theta)$  and a linear predictor  $\mathcal{P}(\Theta)$ , which is only a function of past data, are considered:

$$\mathcal{M}(\Theta) : y(t) = G(q^{-1}; \Theta)u(t) + H(q^{-1}; \Theta)e(t),$$

$$E e(t)e^T(s) = \Lambda(\Theta)\delta_{t,s},$$

$$\mathcal{P}(\Theta) : \hat{y}(t|t-1; \Theta) = L_1(q^{-1}; \Theta)y(t) + L_2(q^{-1}; \Theta)u(t).$$

Here,  $u(t)$  and  $y(t)$  denote the model input and output at time  $t$ .  $\hat{y}(t|t-1; \Theta)$  represents the predicted value of the output at time  $t$ , and  $e(t)$  is white noise. The argument  $q^{-1}$  denotes the backward shift operator, and  $\Theta$  is the model parameter vector. In the prediction-error method, a least-squares minimization is used to determine the model parameter vector  $\Theta$  in such a way that the sum square of the prediction errors

$$\eta(t, \Theta) = y(t) - \hat{y}(t|t-1; \Theta), \quad t = 1, 2, \dots, N,$$

is minimized.

### Identification for robust $H_\infty$ control

A nonlinear system can be modelled as an unstructured set  $\mathcal{S}$  of linear plants. In other words, a nominal model  $P_0(s)$ , a weight  $W(s)$ , and a stable perturbation  $\Delta$  satisfying  $\|\Delta\|_\infty \leq 1$  may be found in such a way that the frequency response of the nonlinear system is represented as<sup>3</sup>  $P(s) = (1 + \Delta(s))$

<sup>3</sup>Perturbations other than multiplicative are also allowed.

$W(s)P_0(s)$ . If a set of identification experiments is performed on the nonlinear system under different operating conditions, the resulting linear frequency response estimates  $P(j\omega)$  will form the set  $P$ . By finding a *nominal fit*  $P_0(j\omega)$  through these frequency response estimates, which reduces the variations among them to a minimum, and encapsulating the whole nonlinearities, disturbances and uncertainties of the system into the perturbation  $\Delta W$ , the information needed for linear  $H_\infty$  controller design are generated. Since  $\|\Delta\|_\infty \leq 1$ ,  $W(j\omega)$  needs to be chosen no smaller than the upper bound of the uncertainty profile at each frequency:

$$\left| \frac{P(j\omega)}{P_0(j\omega)} - 1 \right| \leq W(j\omega), \quad \forall \omega. \quad (7)$$

The details of each step of this nonparametric identification scheme as applied to the RTAC system is reported next.

## 5.2. Simulation study

Prior to identification of the actual system in practice, a simulation study is done based on the nonlinear system of Section 2 to test the effectiveness of the proposed approach. In simulations, it was found that the knowledge of the linearized system can greatly help to overcome possible difficulties during identification. One such difficulty for which simulations were done was the handling of the varying DC gain of the transfer function in (4). The DC gain which varies with the arm angle  $\theta_0$  can reduce the accuracy of the frequency response estimates, because for different operating conditions of the pendulum, the optimization is bound to converge to different local minima. A well-conditioned solution to this problem, as shown in Fig. 3, is to identify only that portion of transfer function (4) which is time invariant<sup>4</sup>, i.e.,

$$\frac{y(t)}{\tilde{x}(t)} = \frac{\varepsilon}{(\varepsilon^2 \cos^2 \theta_0 - 1)s^2 - \frac{\nu}{\sqrt{k(M+m)}}s - 1},$$

and then put the term  $\cos \theta_0$  back to get the actual transfer function using the  $\theta$  values obtained from the system.

For identification tests, a concatenation of positive and negative multisines is used as the excitation input<sup>5</sup>. The reason is that a multisine signal demonstrates a rich and almost uniform spectrum over the frequency range of interest and is highly persistent excitation (*pe*) as the sum of  $n$  sinusoids is *pe* of an order not

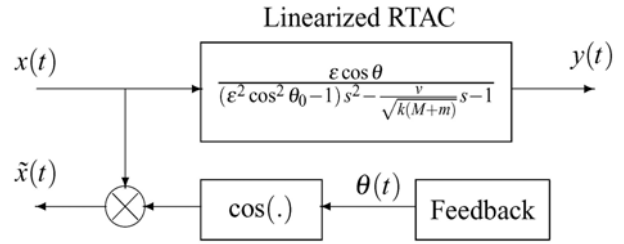


Fig. 3. Compensation of the varying DC gain.

less than  $2n - 2$  [19].

Despite the requirement that the identification input, motor torque, should be limited to  $|N| \leq 0.1$  N.m., it must be able to stimulate the states of the system and to excite all nonlinearities under a wide range of operating conditions. For this purpose, it is essential to select the frequency range within which the excitation input needs to be *pe*, and the distribution of the amplitude and phase of the sinusoids over this frequency range. As it can be seen from (4), the magnitude of the normalized system transfer function is much larger around  $\omega_0 = 1$  rad/s than other frequencies ( $\varepsilon$  and  $\nu$  are small) and, consequently, the system output is less sensitive to harmonics other than  $\omega_0$ . In order to normalize the distribution of amplitudes over the frequencies, the spectral content of the multisine is divided by the magnitude of the linearized system frequency response at each frequency. As a result, the harmonics of the normalized multisine will be equally pronounced at the output.

The amplitude of the input excitation signal is adjusted through experiments such that the output remains within the admissible limits of cart travel, yet it covers all the workspace of the system confirming that the states are persistently excited. It was found through the simulation study that, in this particular problem, detrending the input-output data<sup>6</sup> reduces the accuracy of the frequency response estimates at low frequencies and, therefore, was avoided. Indeed, as discussed in [21], subtracting the mean from nonlinear data can cause a steady-state offset in the model (i.e. poor low frequency estimation) because the mean does not necessarily correspond to the operating point around which a nonlinear system is being perturbed. Identification is performed using both the transient and the steady-state responses of the system. Following the identification, residuals are checked to make sure they are within confidence intervals and, therefore, the identification results are valid.

To further verify the identification, the responses of the nonlinear system, the linearized system given by (4) and the identified system to a multisine input are

<sup>4</sup>The poles of (4) change negligibly with  $\theta_0$ .

<sup>5</sup>Functions *msinclip* and *msinprep* in the Matlab's Frequency Domain Identification Toolbox (FDIDENT) [20].

<sup>6</sup>Subtracting the means from the data.

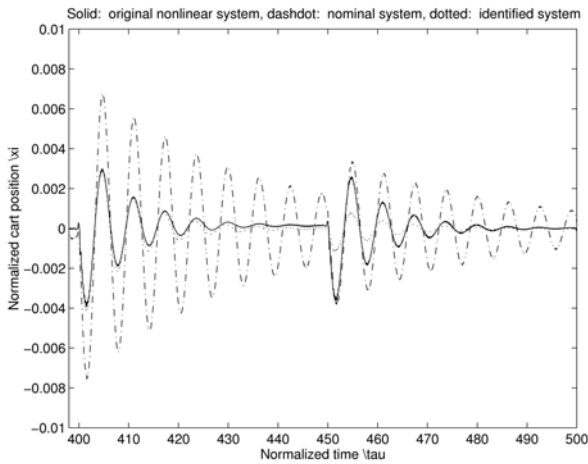


Fig. 4. Response of the nonlinear system (solid), linearized system (dash-dot) and identified system (dotted) to a multisine input during simulations.

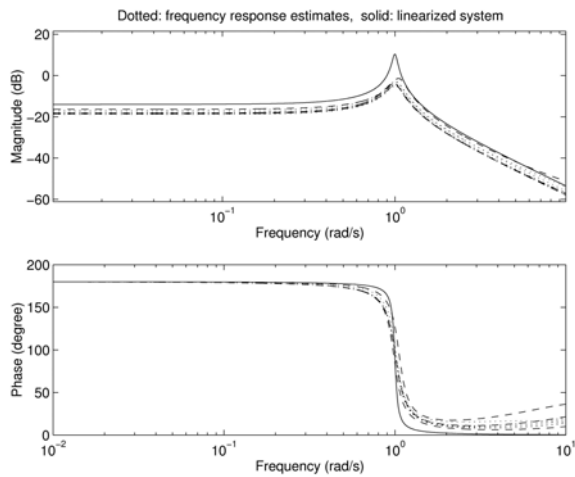


Fig. 5. Frequency response of the estimated and nominal systems during simulations.

shown in Fig. 4. The identified system demonstrates a response much closer to the nonlinear system compared to the linearized system. The occasional discrepancies between the amplitudes of the nonlinear and identified systems outputs can be explained by the fact that, while the nonlinear system frequency response experiences expected variations for different operating conditions, the identified system represents an *average* fixed linear model that, only together with an *uncertainty block*, can fully explain the behavior of the nonlinear system.

Frequency response estimates resulted from prediction-error identification for various operating conditions in addition to the frequency response of the linearized system are illustrated in Fig. 5. The uncertainty profile  $|\frac{P(j\omega)}{P_0(j\omega)} - 1|$  has an upper magnitude limit of  $-10$  dB at low frequencies. This shows that not only the RTAC nonlinear system is

represented by an average linear model and uncertainty, but also the low values of uncertainty at low frequencies promise the effectiveness of  $H_\infty$  synthesis in order to achieve a robust performance for the closed-loop system.

### 5.3. Experimental results

By applying the methods developed in the simulation study of Section 5.2 including the compensation of the varying DC gain and the excitation input selection, we proceed to the experimental identification of the RTAC system. Identification tests are done on the actual system for different initial conditions (i.e. different arm angles) such that the estimated transfer functions are valid representatives of the nonlinear system all over the workspace. The amplitudes of the multisine range from 50% to 100% of their maximum value, with the maximum value being where the limits of cart travel are violated. Since the RTAC system is uncontrollable at  $\theta_0 = \pm 90^\circ$ , the excitation input is taken to be zero when  $\cos \theta_0$  nears zero, e.g. when  $|\cos \theta_0| \leq 0.05$ . Within this uncontrollable span and in the absence of an input, the arm momentum of inertia passes the arm through this region. Finally, the prediction-error minimization is initialized with a parameter vector  $\Theta$  specifying the model structure of the linearized model (4).

The resultant frequency response estimates as well as the frequency response of the selected average (nominal) system  $P_0(s)$  are shown in Fig. 6(a) where

$$P_0(s) = 3.7 \times 10^{-3} \times \frac{(s - 175.7)(s + 32.7)(s + 14.5 \pm j26.6)}{(s + 2.7 \pm j12.9)(s + 4.1 \pm j37.4)}.$$

While the magnitudes of the frequency response estimates experience two peaks at 12.9 rad/s and 37.4 rad/s, our simulation study had previously shown the first peak only (see Fig. 5). The reason for this is that the flexible beams used to realize the springs in the experimental setup form a spring-mass-spring-mass system that has one rigid and one flexible modes. The peak at 12.9 rad/s corresponds to the rigid mode of the mechanical structure, while the 37.4 rad/s harmonic represents the fundamental frequency of the flexible structure.

The uncertainty profile  $|\frac{P(j\omega)}{P_0(j\omega)} - 1|$  and the uncertainty weighting function selected as

$$W(j\omega) = 0.55 \frac{(\frac{j\omega}{2} + 1)(\frac{j\omega}{80} + 1)}{(\frac{j\omega}{5} + 1)(\frac{j\omega}{1000} + 1)} \quad (8)$$

are depicted in Fig. 6(b). For best fulfillment of  $H_\infty$



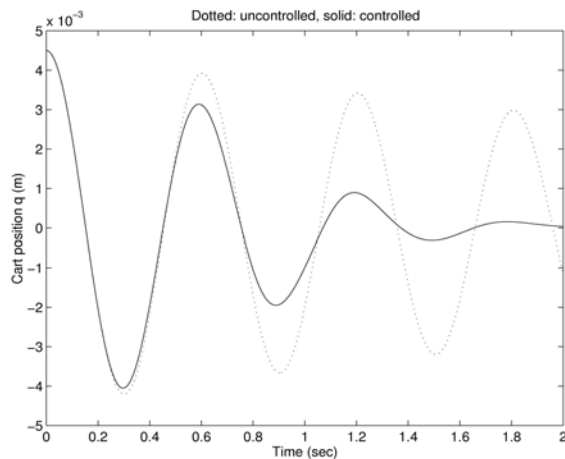


Fig. 8. Responses of the open-loop (dotted) and the closed-loop (solid) systems.

linear system  $P_0(s)$  and the uncertainty weighting functions  $W_1(s), W_2(s), W_3(s)$  and  $W_d(s)$ , all the information needed for designing a linear  $H_\infty$  controller for the RTAC nonlinear system are provided.

Open-loop and closed-loop simulations based on the actual estimated system (Table 1(c)) and the designed  $H_\infty$  controller are set up, with the results depicted in Fig. 8. As it is seen, in response to the natural oscillations caused by the nonzero initial position of the cart, while the uncompensated system shows a poor settling behavior, the  $H_\infty$  controller stabilizes the closed-loop system quite effectively. The control effort is also well between the admissible limits. Therefore, the robust  $H_\infty$  control design is entirely successful in satisfying the required control objectives based on the estimation of the nonlinear system as a linear uncertain system. The results show the success and effectiveness of the proposed approach in dealing with a system that demonstrates extreme nonlinearities due to the coupling between the translational and rotational motions.

## 6. CONCLUSIONS

The RTAC benchmark problem investigates the utility of a rotational actuator for stabilizing translational motion. In this paper, system parameters were estimated in a least-squares framework based on free- and forced-oscillation identification experiments. On the other hand, the control requirements lend themselves well to the robust control synthesis framework. A time-domain nonparametric identification method was used by which the nonlinear system was modelled as a nominal linear system plus uncertainty. It was confirmed in practice that the deviations of the nonlinear system from the average linear system can successfully be condensed into a

small perturbation block. An effective mixed-sensitivity problem that uses the average model and uncertainty information was developed to satisfy all performance requirements as well as robust stability despite actuator saturation.

## REFERENCES

- [1] R. J. Kinsey, D. L. Mingori, and R. H. Rand, "Nonlinear controller to reduce resonance effects of a dual-spin spacecraft through precession phase lock," *Proc. of the 31st Conference on Decision and Control*, pp. 3025-3030, 1992.
- [2] R. T. Bupp, D. S. Bernestein, and V. T. Coppola, "A benchmark problem for nonlinear control design: Problem statement, experimental testbed, and passive nonlinear compensation," *Proc. of American Control Conference*, pp. 4363-4367, 1995.
- [3] D. K. Linder, T. P. Celano, and E. N. Ide, "Vibration suppression using a proofmass actuator operating in stroke/force saturation," *Journal of Vibrations and Control*, vol. 113, pp. 423-433, 1991.
- [4] R. T. Bupp, D. S. Bernestein, and V. T. Coppola, "Experimental implementation of integrator backstepping and passive nonlinear controllers on the RTAC testbed," *Proc. of the IEEE International Conference on Control Applications*, pp. 279-284, 1996.
- [5] M. Jankovic, D. Fontaine, and P. V. Kokotovic, "TORA example: Cascade- and passivity-based control designs," *IEEE Trans. on Control Systems Technology*, vol. 4, no. 3, pp. 292-297, 1996.
- [6] I. Kanellakopoulos and J. Zhao, "Tracking and disturbance rejection for the benchmark nonlinear control problem," *Proc. of American Control Conference*, pp. 4360-4362, 1995.
- [7] Z. P. Jiang and I. Kanellakopoulos, "Global output-feedback tracking for a benchmark nonlinear system," *IEEE Trans. on Automatic Control*, vol. 45, no. 5, pp. 1023-1027, May 2000.
- [8] C. P. Mracek and J. R. Cloutier, "A preliminary control design for the nonlinear benchmark problem," *Proc. of the IEEE International Conference on Control Applications*, pp. 265-272, 1996.
- [9] I. Kolmanovsky and N. H. McClamroch, "Hybrid feedback stabilization of rotational-translational actuator (RTAC) system," *International Journal of Robust and Nonlinear Control*, vol. 8, no. 4-5, pp. 367-375, April 1998.
- [10] W. M. Haddad and V-S. Chellaboina, "Nonlinear fixed-order dynamic compensation for passive systems," *International Journal of Robust and Nonlinear Control*, vol. 8, no. 4-5, pp. 349-365,

April 1998.

- [11] S. Dussey and L. El-Ghaoui, "Measurement scheduled control for the RTAC problem: An LMI approach," *International Journal of Robust and Nonlinear Control*, vol. 8, no. 4-5, pp. 377-400, April 1998.
- [12] P. Tsiotras, M. Corless, and M. A. Rotea, "An  $L_2$  disturbance attenuation solution to the nonlinear benchmark problem," *International Journal of Robust and Nonlinear Control*, vol. 8, no. 4-5, pp. 311-330, April 1998.
- [13] M. Abrishamchian, H. D. Taghirad, and S. M. A. Tavakoli, "Identification for control of a rotational/translational actuator," *Proc. of the 7th Iranian Conference on Electrical Engineering*, pp. 69-76, 1999.
- [14] H. D. Taghirad and P. R. Belanger, "Modeling and parameter identification of harmonic drive systems," *ASME Journal of Dynamic Systems, Measurements, and Control*, vol. 120, no. 4, pp. 439-444, December 1998.
- [15] *Signal Processing Toolbox*, <http://www.mathworks.com/access/helpdesk/help/toolbox/signal>, The MathWorks Inc., 2005.
- [16] H. D. Taghirad and P. Belanger, " $H_\infty$ -based robust torque control of harmonic drive systems," *ASME Journal of Dynamic Systems, Measurement, and Control*, vol. 123, pp. 338-345, September 2001.
- [17] S. Toffner-Clausen, *System Identification and Robust Control: A Case Study Approach*, ser. Advances in Industrial Control (Editors: M.J. Grimble, M.A. Johnson), Springer, 1996.
- [18] M. Namvar and F. Aghili, "A combined scheme for identification and robust torque control of hydraulic actuators," *ASME Journal of Dynamic Systems, Measurement, and Control*, vol. 125, pp. 595-606, December 2003.
- [19] T. Soderstrom and P. Stoica, *System Identification*, Prentice Hall International Ltd, 1989.
- [20] I. Kollar, *Frequency Domain System Identification Toolbox*, The MathWorks Inc., 1994.
- [21] W. A. Docter and Christos Georgakis, "Identification of reduced order average linear models from nonlinear dynamic simulations," *Proc. of American Control Conference*, pp. 3047-2052, 1997.



**Mahdi Tavakoli** received the B.Sc. and M.Sc. degrees in Electrical Engineering from Ferdowsi University and K. N. Toosi University of Technology, Iran in 1996 and 1999. From 1999 to 2001, he worked at Shahrood University, Iran as a lecturer and at Niroo Research Institute, Iran as a research engineer. At present, he is a

doctoral student in the Department of Electrical and Computer Engineering at the University of Western Ontario. His research interests are in identification and control of dynamical systems, developing robotic instruments and surgeon-robot interfaces for medical interventions, and force sensing/feedback for haptics-based teleoperation during robot-assisted surgery and therapy.



**Hamid D. Taghirad** received the B.Sc. degree in Mechanical Engineering from Sharif University of Technology, Tehran, Iran, in 1989, the M.Eng. in Mechanical Engineering in 1993, and the Ph.D. in Electrical Engineering in 1997, both from McGill University, Montreal, Canada. He is an Assistant Professor with the Electrical Engineering

Department, and the Director of the control group and the Advanced Robotics and Automated System (ARAS) research center at K.N. Toosi University of Technology, Tehran, Iran. His publications include two books, and more than 50 papers in international Journals and conference proceeding, and his research interest are robust and nonlinear control applied on the robotic systems.



**Mehdi Abrishamchian** received the Ph.D. degree in Electrical and Computer Engineering from University of Wisconsin, Madison in 1994. He is currently an Actuator Control Technical Lead at Maxtor Corporation in Shrewsbury, MA. His current research interests include robust control analysis and synthesis, applied digital control, and servo-mechanical optimal control.